Corresponding Author: Mr. Ross F. Nelson,

Corresponding Author's Institution:

First Author: Kenneth J Ranson, PhD

Order of Authors: Kenneth J Ranson, PhD; Paul M Montesano, MS; Ross F. Nelson

Research Highlights:

Object-based mapping of the circumpolar taiga-tundra ecotone with MODIS tree cover

- MODIS Vegtation Continuous Fields data used to map northern transition.

- Circumpolar northern boreal transition from taiga to tundra mapped as an ecotone.

- Compare MODIS transition zone to 2 tree lines and Canadian Landsat % tree cover map:
  - Tree line 1 – CAVM: corresponds to 1- 23% MODIS % tree cover.
  - Tree line 2 – CAPI: corresponds to 1-12% MODIS % tree cover.
  - MODIS-Landsat differences of ~25% (worst case) demonstrated.

1 <u>**Object-based mapping of the circumpolar taiga-tundra ecotone**</u>
2 <u>**with MODIS tree cover**</u>
3
4 K.J. Ranson[a], P.M. Montesano[b], and R. Nelson[a,c]
5
6 *a.* Code 614.4, Biospheric Sciences Branch, NASA/Goddard Space Flight Center, Greenbelt, Maryland
7 20771, USA
8 *b.* Sigma Space Corp., Lanham, MD,20706 USA
9 *c.* corresponding author: email: <u>Ross.F.Nelson@nasa.gov</u>, telephone: 1-301-614-6632
10
11 **Abstract**

12   The circumpolar taiga-tundra ecotone was delineated using an image

13 segmentation based mapping approach with multi-annual MODIS Vegetation Continuous

14 Fields (VCF) tree cover data. Circumpolar tree canopy cover (TCC) throughout the

15 ecotone was derived by averaging MODIS VCF data from 2000 - 2005 and adjusting the

16 averaged values using linear equations relating MODIS TCC to Quickbird-derived tree

17 cover estimates. The adjustment helped mitigate VCF's overestimation of tree cover in

18 lightly forested regions. An image segmentation grouped pixels representing similar tree

19 cover into polygonal features (objects) that form the map of the transition zone. Each

20 feature represents an area much larger than the 500m MODIS pixel to characterize the

21 patterns of sparse forest patches on a regional scale. Comparisons of the adjusted average

22 tree cover data were made with (1) two existing tree line definitions aggregated for each

23 1° longitudinal interval in North America and Eurasia and (2) Landsat-derived Canadian

24 proportion of forest cover for Canada. The adjusted TCC from MODIS VCF shows, on

25 average, <12% TCC for all but one regional zone at the intersection with independently

26 delineated tree lines. Adjusted values track closely with Canadian proportion of forest

27 cover data in areas of low tree cover. Those polygons near the boreal/tundra interface

28 with either (1) mean adjusted TCC values between 5-20% , or (2) mean adjusted TCC

29 values <5% but with a standard deviation > 5% were used to identify the ecotone.

Introduction

Earth's longest vegetation transition zone, the circumpolar taiga-tundra ecotone

(TTE), stretches for more than 13,400 km around Arctic North America, Scandinavia,

and Eurasia (Callaghan et al. 2002a). This ecotone is subjected to climate change

(Serreze et al. 2000), and sensitive to climate change (Callaghan et al. 2002b). The

shifting of local subarctic tree lines throughout the forest-tundra biome is linked to

ecological processes at different spatiotemporal scales and will reflect future global

climatic changes (Payette et al. 2001). Monitoring the dynamics of this forest-tundra

boundary is critical for our understanding of the causes and consequences of the changes.

High-latitude ecosystems, i.e. boreal forests and tundra, play an important role in the

climate system (Bonan et al. 1995) and have been warming in recent decades (Chapin et

al. 2005). Modeled effects of increased deciduous tree cover in high-latitudes show a

positive feedback with temperature in the vegetated regions of the arctic (Swann et al.

2010). Improved understanding of the role of the forest-tundra boundary requires a

concerted research effort to be conducted over a long enough time period to detect and

quantify ecosystem feedbacks (Chapin et al. 2000).   The objective of this study was to

develop a framework for long term monitoring of the circumpolar tundra-taiga ecotone

using satellite data. We accomplish this by preparing a validated map of MODIS percent

forest cover for the entire ecotone with repeatable methods. This goal is to provide a

benchmark for future studies of the tundra-taiga ecotone. We accomplish this by

preparing a validated map of MODIS percent forest cover for the entire ecotone using

52   procedures easily replicated by others. The results provide a benchmark for future

53   studies of the tundra-taiga ecotone.

54

55   **Background**

56   The TTE is dynamic because it is very sensitive to human activity and climate

57   change. For example, during the last 6000 years in northern Eurasia a general cooling

58   trend of about 2-4°C was associated with a 400 – 500km southward retreat of larch and

59   birch forest stands (Callaghan et al. 2002b). In the past three decades global average

60   surface air temperatures have risen by approximately 0.6^{o}C (Hansen et al. 2006) while

61   temperatures in parts of the Northern Hemisphere have warmed by as much as 2°C

62   (Hansen et al. 1999). If it is assumed that growth and reproduction are controlled by

63   temperature, a rapid advance of the tree line would be predicted (Grace et al. 2002). The

64   northward movement of the TTE may result if climatic warming persists over centuries

65   or millennia (Skre et al. 2002). Some studies predict that up to about one half of the

66   tundra could be colonized by trees by 2100 (Callaghan et al. 2002b; Harding et al. 2001).

67   There is general agreement that temperature is important in determining the

68   northern extent of the boreal forest. Widespread degradation of permafrost has been

69   shown in numerous studies (Pavlov 1994; Osterkamp and Romanovsky 1996; Osterkamp

70   and Jorgenson 2006; Jorgenson et al. 2006). Recent observations suggest that, in an

71   indication of northern climate warming, shrubs and forests are expanding into the tundra

72   (e.g., Kharuk et al. 1998, 2002; Esper and Schweingruber 2004; Tape et al. 2006; Blok et

73   al. 2010) and experimental evidence shows that increased shrub cover in the tundra is a

74   response to warming (Walker et al. 2006). In a case study conducted by Rees et al.

75   (2002) in a portion of the West Siberian plain (66.5°N, 70.75°E) from 1968 to 1997,

76   seven of their 20 test sites showed colonization by advancing forests, one showed an

77   inconclusive shift in the tree line and one test site, which was surrounded by water and

78   wetlands, showed evidence of forest retreat. The remaining 11 sites showed no

79   appreciable forest advance but four of these sites had developed denser forest cover. In

80   the Polar Ural mountains crown closure of stands increased 4-5 times and the tree line

81   boundary shifted 100-300 m into the tundra (Kharuk et al. 1998). Devi et al. (2008)

82   estimate the past century's forest expansion in this region has led to an increase in

83   biomass of 40-75 Mg/ha. These observations are consistent with those in northern

84   Canada (Payette and Gagnon 1985) while transects through the forest-tundra in eastern

85   Canada have shown no significant correlations in the short term (5-20 years) with

86   climatic variables, but do reveal a rise in tree line (Gamache and Payette 2005). In the

87   TTE in western, central and eastern Canada white spruce density increased without any

88   significant displacements of the Arctic tree line over the past 100-150 years (Payette et al.

89   2001). Recently established trees near the forest limit at coastal sites east of Hudson Bay

90   are associated with warmer conditions over the past 100 years (Laliberté and Payette

91   2008). However, from the 1970s – 1990s, a Landsat-based study of the TTE in two areas

92   of northern Canada has also shown that the extent of the boreal forest in these areas

93   remain stable (Masek 2001). It is important to note that the position of northern portion of

94   the boreal forest is likely influenced by a range of conditions that vary by region

95   (Callaghan et al. 2002a; Crawford and Jeffree 2007; Crawford 2005).

96   Recent work indicates increased Arctic vegetation growth with climate warming.

97   Experiments have shown that a 1-3°C temperature warming can increase the height and

98 cover of deciduous shrubs in the tundra after two growing seasons (Walker et al. 2006).

99 Analysis of shrub growth rings in northwestern Russian Arctic tundra has revealed field

100 data that closely follows the patterns found in the greening signal of shrubs in the satellite

101 record since the 1980s (Forbes et al. 2010). Results from the analysis of Landsat time

102 series in Canada's forest-tundra interface suggests shrub replacement of bare ground and

103 lichen cover (Olthof et al. 2008). Kharuk et al. (2005) studied the expansion of evergreen

104 conifers into larch-dominated forest, noting the increase in tree-stand density and the

105 spread of larch in the ecotone. However, the patterns of vegetation growth may not be

106 consistent across the taiga-tundra transition (Bunn and Goetz 2006; Verbyla 2008) or

107 may be interpreted differently depending on the scale of the analysis (Alcaraz-Segura et

108 al. 2010). Furthermore, vegetation change may in many cases depend on site-specific

109 characteristics, particularly where there is a direct effect from human activities (Crawford

110 et al. 2003; Virtanen et al. 2002; Vlassova 2002; Toutoubalina and Rees 1999; Rees et al.

111 2002; Hagner and Rigina 1998).

112 The transition from taiga to tundra is characterized by a change in tree cover

113 density. The TTE is not a distinct edge but a transition area where patches of tundra and

114 forest are mixed. It is not easily defined and can be difficult to identify and quantify.

115 Timoney et al. (1992) described the TTE in Canada in terms of the ratio forest to tundra

116 identified on aerial photographs and Timoney (1995) highlights major differences in the

117 ecotone from west to east. Across the circumpolar ecotone the abundance of trees has

118 been used to identify vegetation patterns and monitor these patterns for shifts indicative

119 of vegetation's response to human activities and climate changes. Rees et al. (2002)

120 discuss identifying and monitoring the TTE in Russia using Landsat and Synthetic

121   Aperture Radar (SAR) data and the potential and limitations associated with satellite

122   observation. Esper and Schweingruber (2004) suggest that there is a circumpolar trend of

123   changes in treeline occurring where there are notable temperature changes and consistent

124   monitoring methods are needed (Frey and Smith 2007). Spectral un-mixing methods

125   (Sun et al. 2004) and multi-angular and –temporal data (Heiskanen and Kivinen 2008)

126   have been used to characterize tree cover in the TTE. Stow et al. (2004) discuss multi-

127   temporal remote sensing of land cover change applications in the Arctic, presenting case

128   studies with a range of spatial resolutions and extents with durations spanning months to

129   decades. These studies have shown that the climatically induced changes in vegetation

130   cover and composition in the Arctic need to be monitored at different spatial scales.

131   Ranson et al. (2004) examined the capabilities of remote sensing data for identifying the

132   tundra-taiga transition zone in Ary-mas, Siberia by mapping the tree abundances. Their

133   results showed that Landsat-7 ETM+ image and C-band SAR (RADARSAT) were

134   adequate for mapping tree density in this area. They also demonstrated that lower

135   resolution data such as MODIS can also be used to characterize the transition zone when

136   adequate training data are available.

137   Image segmentation has been used with MODIS data (Tilton et al. 2006) and to

138   delineate forest features and analyze forested areas at multiple scales (Pekkarinen 2002;

139   van Aardt et al. 2006; Achard et al. 2009). Segmentations of high resolution digital aerial

140   imagery were used to delineate vegetation (seagrass) percent cover (Lathrop et al. 2006).

141   The purpose of this technique is to group pixels into meaningful image objects that

142   represent landscape features. While groups of adjacent remote sensing pixels within a

143   particular land cover category may be similar, they typically exhibit internal

144   heterogeneity. The segmentation process aims to minimize internal segment (image

145   object) heterogeneity by accounting for both local image texture and the size of groups of

146   pixels (Baatz and Schäpe 2000). Image segmentation procedures are useful for

147   characterizing boundaries between ecological regions, where patches of vegetation of

148   varying densities and gaps can signal a transition between land cover types. McMahon et

149   al. (2004) suggest that research on ecological regions should consider the hierarchical

150   relationship of landscape elements. The mean and variance associated with individual

151   image objects, coupled with the hierarchical relationship of objects and sub-objects can

152   be used to quantify changes in vegetation patches and gaps across a geographic gradient.

153   Furthermore, the segmentation process can facilitate remote sensing data fusion, by

154   incorporating information from multiple datasets on a per-segment basis.

155

156   **Methods**

157   *MODIS data acquisition and processing*

158   Figure 1 is a composite Terra MODIS image of the northern hemisphere above

159   50° latitude. This image represents the geographic scope and diversity in the vegetated

160   boreal and arctic zones. Collection 4 (C4) MODIS VCF (MOD44b) data (USGS

161   LPDAAC 2010) was acquired as 10° x 10° tiles for 6 years (2000 – 2005) for the 21 tiles

162   shown in Figure 2. Tiles for continental North America spanned 50°N – 70°N and tiles

163   for Eurasia spanned 60°N - 70°N. No C4 MODIS VCF data existed above 70°N, which

164   accounts for the data gap in northern Siberia.   The data tiles were mosaicked by year for

165   both North America and Eurasia using ENVI 4.5 software (ENVI 2010). The 6 years of

166   data were then combined to derive an average VCF dataset, where each pixel represented

167 the mean percent tree canopy cover value of the corresponding pixel across all of the 6

168 VCF yearly datasets. Finally, the Collection 5 MODIS land cover (MCD12Q1, IGBP

169 global vegetation classification scheme) was used to change those VCF pixels whose

170 corresponding land cover type was water to tree canopy cover values of zero. Two multi-

171 annual datasets, one for continental North America and one for Eurasia resulted from this

172 processing sequence, each maintaining the original sinusoidal projection of the 463.3m

173 (nominally 500m) pixel grid.

174 *VCF Adjustment*

175   Each continental multi-annual VCF mosaic was adjusted based on inversions of

176 the results of linear regressions, shown in Table 1, relating Quickbird-validated percent

177 tree cover to MODIS VCF percent tree canopy cover (Montesano et al. 2009).   The

178 adjustments were applied for seven broad longitudinal zones representing very general

179 circumpolar regions on a pixel-by-pixel basis (Figure 3). A value of zero was assigned to

180 those pixels for which the adjustment equations resulted in negative values, while a value

181 of 100 was assigned to those pixels whose adjusted values exceeded 100 percent tree

182 canopy cover.

183   The tree canopy cover values for pixels of the adjusted multi-annual VCF mosaics

184 (VCF_{adj}) were examined within the taiga-tundra ecotone using two existing definitions of

185 tree line. Vector polylines, approximating the northern limit of trees, from both the

186 Circumpolar Arctic Vegetation Map (CAVM) (Walker et al. 2005) and the Circum-Arctic

187 Map of Permafrost and Ground-Ice Conditions (CAPI) (Heginbottom et al. 1993) were

188 decomposed into points at intervals of 463.3m (the size of a VCF pixel). These points

189 were used to sample corresponding VCF_{adj} pixels within one-degree longitudinal

190   intervals wherever the points overlay VCF_{adj} pixels. The VCF pixel-sized interval was

191   used to avoid oversampling any single VCF pixel and risk skewing the mean VCF value

192   in 1° interval. For each 1° interval, the mean VCF_{adj} value for all VCF_{adj} pixels

193   intersecting the sampling points from both the CAVM and the CAPI treelines were used

194   to determine the mean VCF_{adj} TCC at each treeline.

195   VCF_{adj} canopy cover was examined using data from the Canadian Forest Service

196   of Natural Resources Canada. The dataset is a 1km derived product of the Earth

197   Observation for Sustainable Development of Forests land cover products (EOSD)

198   (Wulder et al. 2008). The value of each 1km grid cell represents the proportion of the

199   cell occupied by the within-cell majority EOSD class. For the 2 broad circumpolar zones

200   in which Canada lies, a zonal mean analysis was performed to compare proportion of

201   forest values at 1 km (from EOSD) to mean TCC values from the VCF_{adj}. For each

202   EOSD value from 0 – 100% forest cover, we computed the median VCF_{adj}.

203   *VCF Segmentation*

204   To further mitigate pixel-level noise in the relationship of VCF tree canopy cover

205   and Quickbird-based validation of tree cover in the TTE, groups of similar adjacent

206   pixels were aggregated in a segmentation process. The segmentation algorithm minimizes

207   within-object variance by arranging groups of spectrally similar, adjacent pixels into

208   polygon image objects, or segments. The segmentation was applied to both the North

209   American and the Eurasia adjusted VCF mosaics. To facilitate processing, each mosaic

210   was divided into tiles. North America was divided into three tiles, where the largest was

211   4600 pixels X 4800 pixels, while Eurasia was divided into 5 tiles, where the largest tile

212   was 5000 pixels X 2400 pixels.

213   In addition to the VCF_{adj} raster dataset, vector layer datasets were used as masks

214   to constrain the segmentations to land areas within previously delineated taiga and tundra

215   biomes. The World Wildlife Fund's (WWF) Global Lakes and Wetlands Database

216   (Lehner and Doll 2004) was used to apply a water mask to the VCF_{adj} mosaics for all

217   water polygons labeled "lake", "river", or "reservoir" and complemented the water mask

218   provided by the MODIS IGBP scheme. The WWF's Ecoregions (Olsen et al. 2001)

219   vector dataset depicts global terrestrial ecoregions defined as large land units comprised

220   of distinct species and natural communities.   All ecoregions within the Boreal

221   Forests/Taiga biome and the Tundra biome were included in the vector masking portion

222   of the overall segmentation procedure.

223   The segmentation process involved two steps. The steps were arranged in a

224   protocol to standardize the processing steps for each tile of the VCF_{adj}. The first step

225   involved an initial coarse segmentation allowing the vector layers to mask portions of the

226   VCF_{adj} land pixels that were outside the Boreal Forest/Taiga or Tundra biomes.

227   Subsequent class assignments, masking and segmentations were performed based on the

228   masks established in this first step. The second step, applied within the mask area,

229   created image objects using consistent scale parameter and homogeneity criterion. The

230   scale parameter guides the general size of the image objects, and depends on the

231   homogenous nature of pixel values in an area (Baatz and Schäpe 2000). The more

232   homogenous the data, the larger the objects tend to be. The goal of this segmentation

233   procedure was to derive image objects that represented various tree cover (forest)

234   patches, identifying gaps of little to no tree cover, and delineating landscape objects with

235   varying tree cover densities. The homogeneity criterion is comprised of complementary

236   color and shape components. Eighty percent of the weight was given to the color

237   component, which is associated with the digital value of the pixels. The shape

238   component, which defines the textural homogeneity of the resulting image objects,

239   received the remaining 20%.

240   *Taiga-Tundra Ecotone Mapping*

241   The mapping portion was accomplished by classifying image objects based on a

242   specified range of image object values that represent the TTE.   For each image object,

243   mean and standard deviation were calculated and attributed. The mean and standard

244   deviation values were derived from the VCF_{adj} pixels that make up the image object.

245   Image objects, whose sizes ranged widely depending on the nature of local VCF_{adj} value

246   homogeneity, were considered part of the TTE if they fit one of the following two

247   criteria:

248   1.   The mean VCF_{adj} value was 5% - 20%.

249   2.   The mean VCF_{adj} value was < 5% and the standard deviation > 5%.

250   Values within the biomes "Boreal Forest/Taiga" and "Tundra" that did not meet these

251   criteria were not considered part of the TTE. Image objects whose mean adjusted value

252   and standard deviation were both less than 5% were considered outside the TTE and

253   classified as tundra while image objects with a mean VCF_{adj} value greater than 20% were

254   not considered part of the TTE, and classified as boreal forest.

255

256   **Results**

257   *Examining the Adjusted VCF*

258   The intersection of VCF_{adj} polygons with two representations of tree-line was

259   produced for the circumpolar ecotone below 70°N. The intersection of the datasets show

260   the correspondence of low VCF_{adj} %TCC values with tree-line in North America and

261   Eurasia compiled for each regional zone (Table 2). The regional zone means are an

262   aggregation of the 1° longitudinal means of the VCF_{adj} values at their intersection with

263   each tree-line. Adjusted values above 20% are reported for the Western Eurasia regional

264   zone (40°E – 60°E), while all other zones average less than 12% VCF_{adj} tree cover at

265   both tree-lines. Most of the regional zones have a mean %TCC less than 5 for at least

266   40% of their 1 degree intervals (5 of 6 of the zones at the CAVM tree line, 6 of 7 at the

267   CAP tree line). This is indicative of agreement among the tree line data and the VCF_{adj}

268   on areas of low %TCC.

269   Plots of mean VCF_{adj} values for each 1° longitudinal zone in North America

270   (Figure 4a) and Eurasia (Figure 4b), show the performance of the VCF_{adj} across the

271   circumpolar transition zone. In North America, particularly west of Hudson Bay, the

272   linear adjustments brought %TCC values to near zero in many longitudinal zones. In

273   Eurasia, VCF_{adj} values are more variable, and spikes in %TC are apparent between 55°E

274   and 80°E. There is a broad gap in Figure 4b between 88°E and 148°E where, for the

275   most part, the CAVM and CAPI tree-lines lie above 70°N, where C4 VCF data was not

276   available. An interruption of the intersection between the tree-lines and the VCF_{adj} also

277   occurs in North America at Hudson Bay.

278   We compared the VCF_{adj} to the EOSD-derived proportion of forest within a 1km

279   x 1km grid cell. The proportion of forest is a product aggregated from the 25m Landsat-

280   based EOSD land cover data for Canada (Wulder et al. 2008). The dataset was provided

281   in the Lambert Conformal Conic projection and was resampled to the sinusoidal

282   projection to match that of the VCF. It covers nearly 6.6 million sq. km., approximately

283   1.7 million of which lie in the Eastern Canada zone and 4.9 of which lie in the Western

284   Canada zone. The dataset accounts for nearly one third of the world's boreal forest, and

285   one tenth of the global forest cover. The median VCF_{adj} value associated with each

286   EOSD 1% bin was plotted for both of Canada's regional zones (Figure 5). Although the

287   VCF_{adj} values range from 0% - 100% for all EOSD bins, the median VCF_{adj} is within an

288   average of 5% TCC between EOSD bins 0-30 for both Eastern and Western Canada. The

289   low %TCC portion of the plot is of particular interest because the adjustment algorithms

290   applied to the VCF were designed for areas of low TCC.

291   The EOSD - VCF_{adj} comparison illustrated in Figure 5 is an approximation

292   because the two products are responding to two different definitions of forest. The

293   VCF_{adj} map reports a 500m pixel, whereas the EOSD map reports percent forest cover in

294   a $1km^2$ cell. The EOSD data reflects the proportion of the $1km^2$ cell occupied by the

295   plurality EOSD class, forest. Exclusion of areas of significant tree/forest cover is

296   possible, when extensive forest cover (e.g. 40%) is eclipsed within a cell by another more

297   dominant land cover comprising the remaining 60% of the cell. In such a case, this

298   particular cell would not be included in the proportion of forest cover product, and thus

299   would not have an effect on this comparison of the two datasets. However, tree cover not

300   reflected in the EOSD forest category can result in the VCF_{adj} showing higher %TCC

301   values than EOSD forest cover values.

302   *The Circumpolar Taiga-Tundra Ecotone Map*

303   The map delineates a global scale circumpolar taiga-tundra ecotone for the base

304   period 2000-2005. The map data is cast in the sinusoidal projection, matching the

305   original projection of the input VCF. In Eurasia, the map extends from 60°N – 70°N, and

306   in North America from 50°N – 70°N, excluding Baffin Island in north-eastern Canada

307   and the Aleutian Peninsula in south-western Alaska. Figure 6a shows the map of the

308   circumpolar TTE in a polar projection. Figures 6b-g show greater detail for each regional

309   zone. These regional maps highlight the variability of the ecotone between regions as

310   well as the patchy nature

311   The data exists in digital GIS format, as both raster GeoTiff files and vector

312   shapefiles. The vector shapefiles contain mean and standard deviation VCF_{adj} percent

313   tree canopy cover values for each ecotone polygon, as well as the area of each polygon in

314   square kilometers. The ecotone is delineated with two classes. Class 1 is comprised of

315   polygons of 5%-20% mean tree canopy cover. Polygons with less than 5% mean tree

316   canopy cover but with a standard deviation greater than 5% make up Class 2. The

317   minimum polygon size for 95% of the TTE objects is 2.5 sq. km., which corresponds to

318   the minimum mapping unit. Greater than 95% of the area mapped as ecotone is

319   comprised of polygons that are at least 20 sq. km. in size.

320   The ecotone, below 70°N, covers over 1.9 million sq. km., 64% of which is found

321   in North America. Table 3 summarizes the area of each ecotone class by regional zone as

322   well as the ratio of Class 1 to Class 2. Regional ecotone areas range widely from 49k –

323   322k sq. km. in Class 1 and from 33k-301k sq. km. in Class 2. This may be largely due

324   to the longitudinal extent of each zone.   The ratio of Class 1 to Class 2 reported in Table

325   3 provides insight into the nature of the transition and may indicate the ability of MODIS

326   to identify taiga-tundra transition across a region using MODIS-level satellite monitoring.

327   Class 2 shows where tree cover may occur at densities too low to be reliably detected by

328   MODIS. Notice the high ratio value for Western / Central Canada, where the ecotone is

329   compact and easily demarcated compared with the low value for Eastern and Western

330   Eurasia where the ecotone is appears more disjoint.

331

332   **Discussion**

333   We use adjusted values of a continuous tree canopy cover values from the

334   MODIS VCF to map the ecotone at the taiga-tundra interface. The adjustment algorithms

335   applied to VCF tree canopy cover pixels were based on validation results for the

336   circumpolar taiga-tundra ecotone. The adjustment decreases the overestimation of tree

337   canopy cover in areas of low tree cover, such as the transition from closed canopy boreal

338   forest to open tundra. The map was created by grouping homogenous, adjacent sets of

339   pixels using image segmentation. Ecotone polygons based on the original 500m pixel

340   data were divided into two classes according to internal mean tree canopy cover and

341   variance. These classes are bounded by a maximum TCC of 20%. This upper bound is

342   consistent with the definition of the lower limit of forest in Potapov et al. (2008), where

343   global intact forest landscapes were mapped using VCF TCC above 20%. The purpose of

344   the segmentation process was to reduce pixel-level scatter, and derive patches of low tree

345   canopy cover. While patches of low VCF_{adj} TCC do not necessarily indicate an ecotone,

346   their proximity to the boundary of the Boreal Forest/Taiga and Tundra biomes help

347   define the collective meaning of groups of patches. These groups of patches illustrate the

348   complex regional variations in the transition from forest to tundra, and identify the

349   circumpolar taiga-tundra ecotone for the 2000-2005 base period.

350   The circumpolar taiga-tundra ecotone map shows regional differences across both

351   North America and Eurasia. In the Central Canada zone (west of Hudson Bay), the map

352   depicts an ecotone that is relatively well defined and show a NW-SE orientation. In this

353   zone, ecotone polygons coalesce revealing a visually identifiable, rapid NE-SW transition

354   of patches of homogenous low tree canopy cover. The steep vegetation gradients of this

355   portion of the ecotone, well documented in Timoney et al. (1992) and Payette et al.

356   (2001), are due to elevation changes, parent material and fire history. Timoney et al

357   (1992) indicate that changes in the width of the ecotone in Canada are also correlated

358   with radiation, climate, and edaphic conditions. The ecotone east of Hudson Bay is more

359   discontinuous, possibly due to trees' difficulty in reproducing after disturbances (Payette

360   and Gagnon 1985, ACIA 2005). Other portions of the circumpolar ecotone, such as the

361   Eastern Eurasia zone, reveal a more fragmented environment where the transition from

362   closed canopy forest to open tundra at the regional scale may be driven by topographical

363   influences.

364   The comparison of the two tree lines with the VCF_{adj} shows good agreement

365   between two representations of the northern extent of tree cover. Since the MODIS-

366   resolution map cannot delineate tree line, we acknowledge the inherent difficulty in

367   comparing the CAVM and CAPI lines with polygons based on groups of 500m pixels.

368   Our method of sampling the VCF_{adj} using points along each tree line spaced at a

369   distances equal to the width of a MODIS pixel provided a good estimate of the

370   performance of the VCF_{adj} at 1° longitudinal intervals. The low mean values in Canada

371 and the relatively higher values in Eurasia are not surprising. The Canadian ecotone is

372 more compact and thus easier to depict with a line. Sections of the ecotone that are more

373 fragmented are less likely to have an easily identifiable tree line. This, in part, may

374 account for some component of the spikes in mean VCF_{adj} value in the 1° zones in

375 Western Eurasia. However, the spikes may be due, in large part, to artifacts of the

376 adjustment. The linear adjustment algorithms were designed to reduce the

377 overestimations of tree canopy cover in areas of low TCC. Where the VCF did not

378 initially identify low tree cover, the VCF_{adj} will show increased %TCC values. This may

379 be occurring in some the longitudinal zones showing spikes in VCF_{adj} relationship with

380 tree line data. These areas should be considered for more local scale refinement.

381 Furthermore, latitude may not be the primary determinant constraining the ecotone

382 throughout the region. Geographic features such as river corridors traversing a north-

383 south gradient through the ecotone may account for significant variations in local tree

384 cover conditions.

385   Although the VCF maps tree canopy cover, there is evidence that the VCF TCC

386 product confuses trees with shrubs (Heiskanen 2008, Gessner et al. 2008, Montesano et

387 al. 2009). As the arctic warms, the increase in shrub cover that is correlated to a greening

388 signal, described by Forbes et al. (2010), may be inadvertently documented by the VCF.

389 The adjustment of the VCF addresses the confusion between shrub and tree cover greater

390 than 5m (Hansen et al. 2003), however some shrub/tree confusion most likely persists.

391   The C4 VCF data gap above 70°N presents a problem where the ecotone extends

392 above this latitude. There are several areas above 70°N where visual inspection of high-

393 resolution multispectral imagery reveals forested patches; northern Scandinavia and

394   Russia's Taimyr Peninsula and Yana River delta.   Documenting these portions of the

395   ecotone is critical. We expect an updated VCF product in late 2010 that will include

396   processing of MODIS tiles above 70°N. We plan to update the ecotone map with those

397   datasets when they become available.

398   This TTE map can be a used in a number of ways. First, it can be included in

399   global models that require forest extent information for the high northern latitudes. The

400   map provides an explicit northern extent for the boreal forest/taiga. Second, when used

401   as a mask the map provides a means by which vegetation structural changes can be

402   monitored. Finally, it may be used as the multispectral component in data

403   integration/fusion studies examining vegetation structure such as height and biomass with

404   finer resolution radar and lidar data.

405

406   **Conclusions**

407   We mapped the circumpolar taiga-tundra ecotone using 500m MODIS VCF data

408   from 2000-2005 adjusted to improve tree canopy cover delineation in areas of low tree

409   cover. The map provides an estimation of the transition between boreal forest/taiga and

410   tundra and is a benchmark for subsequent monitoring. We mapped the ecotone from

411   50°N-70°N in North America and 60°N-70°N in Eurasia with polygons of VCF_{adj} tree

412   canopy cover below 20%. The internal composition of each polygon is characterized by

413   mean and variance values that explain the heterogeneity of the VCF_{adj} pixels that form

414   the polygon classes of tree cover. The first class, covering > 1.3 million sq. km.

415   represents 5-20% adjusted tree canopy cover. The second class, covering >0.6 million

416   sq. km. represents patches of adjusted tree canopy cover <5% with standard deviations

417   >5%.   The minimum mapping unit is approximately 2.5 sq. km., which is the minimum

418   size of 95% of the class 1 and 2 ecotone polygons. Groups of polygons reveal the

419   variability of the ecotone across 7 regional zones. The consistent treatment of the entire

420   circumpolar region facilitates comparisons between regions and use with other global

421   datasets.

422

426

427   **References**
428   ACIA. (2005). Impacts of a Warming Arctic: Arctic Climate Impact Assessment.
429   Cambridge University Press, Cambridge.

430
431   Achard, F., Beuchle, R., Bodart, C., Brink, A., Carboni, S., Eva, H., Mayaux, P., Rasi, R.,
432   Simonetti, D., & Stibig, H.J. (2009). Monitoring forest cover at global scale: the JCR
433   approach, *Proceedings of the 33rd ISRSE conference,* 4 pp.

434
435   Alcaraz-Segura, D., Chuvieco, E., Epstein, H.E., Kasischke, E.S., & Trishchenko, A.
436   (2010). Debating the greening vs. browning of the North American boreal forest:
437   differences between satellite datasets. *Global Change Biology, 16*, 760-770.

438
439   Baatz, M. & Schäpe, A. (2000). Multiresolution segmentation: an optimizing approach
440   for high quality multi-scale image segmentation. In: Angewandte Geographisch
441   Informationsverarbeitung, XII Strobl, J. and T. Blaschke, editors. Wichmann. Heidelberg.
442   pp. 12–23.

443
444   Blok, D., Heijmans, M., Schaepman-Strub, G., Kononov, A.V., Maximov, T.C., &
445   Berendse, F. (2010). Shrub expansion may reduce summer permafrost thaw in Siberian
446   tundra. *Global Change Biology, 16*, 1296-1305.

447
448   Bonan, G.B., Chapin III, F.S., & Thompson, S.L. (1995). Boreal forest and tundra
449   ecosystems as components of the climate system. *Climate Change*. 29, 145-167.

450
451   Bunn, A.G., & Goetz, S.J. (2006). Trends in satellite-observed circumpolar
452   photosynthetic activity from 1982 to 2003: The influence of seasonality, cover type, and
453   vegetation density. *Earth Interactions, 10*, 1-19.

454
455 Callaghan, T.V., Crawford, R.M.M., Eronen, M., Hofgaard, A., Payette, S., Rees, W.G.,
456 Skre, O., Sveinbjornsson, J., Vlassova, T.K., & Werkman, B.R. (2002a). The dynamics of
457 the tundra-taiga boundary: An overview and suggested coordinated and integrated
458 approach to research. *Ambio*, 3-5.
459
460 Callaghan, T.V., Werkman, B.R., & Crawford, R.M.M. (2002b). The tundra-taiga
461 interface and its dynamics: Concepts and Applications. *Ambio,* 6-14.
462
463 Chapin III, F.S., McGuire, A.D., Randerson, J., Pielke Sr., R., Baldocchi, D., Hobbie,
464 S.E., Roulet, N., Eugster, W., Kasischke, E., Rastetter, E.B., Zimov, S.A., & Running,
465 S.W. (2000). Arctic and boreal ecosystmes of western North America as components of
466 the climate system. *Global Change Biology.* 6(1), 211-223.
467
468 Chapin III, F. S., Sturm, M., Serreze, M. C., McFadden, J. P., Key, J. R., Lloyd, A. H.,
469 McGuire, A. D., Rupp, T. S., Lynch, A. H., Schimel, J. P., Beringer, J., Chapman, W.
470 L., Epstein, H. E., Euskirchen, E. S., Hinzman, L. D., Jia, G., Ping, C. L., Tape, K. D.,
471 Thompson, C. D. C., Walker, D. A., and Welker, J. M. (2005). Role of land-surface
472 changes in Arctic summer warming, Science*, 310, 657–660.
473
474 Crawford, R.M.M. (2005). Trees by the sea: advantages and disadvantages of oceanic
475 climates. Proceedings of the Royal Irish Academy, 105B, 129-139.
476
477 Crawford, R.M.M. & Jeffree, C.E. (2007). *Northern climates and woody plant
478 distribution*. In "Arctic-alpine ecosystems and people in a changing environment" (ed.
479 J.B. Orbaek, R Kallenborn, I Tombre, EN Hegseth, S Falk-Petersen, AH Hoel), pp. 85-
480 104. Springer Verlag, Berlin ISBN- 10 3-540-48512-4 and ISBN-13 978-3-540-48512-4
481
482 Crawford, R.M.M., Jeffree, C.E., & Rees, W.G. (2003). Paludification and forest retreat
483 in northern oceanic environments. *Annals of Botany*, 91(2), 213-226.
484 doi:10.1093/aob/mcfl85
485
486 Devi, N., Hagedorn, F., Moiseev, P., Bugmann, H., Shiyatov, S., Mazepa, V. & Rigling,
487 A. (2008). Expanding forests and changing growth forms of Siberian larch at the Polar
488 Urals treeline during the 20th century (pages 1581–1591), Global Change Biology, 14(7),
489 1455–1702. DOI: 10.1111/j.1365-2486.2008.01583.x
490
491 Esper, J., & Schweingruber, F.H. (2004). Large-scale treeline changes recorded in
492 Siberia. *Geophysical Research Letters, 31*, 1-5.
493
494 Forbes, B.C., Fauria, M.M., & Zetterberg, P. (2010). Russian Arctic warming and
495 'greening' are closely tracked by tundra shrub willows. *Global Change Biology, 16*, 1542-
496 1554.
497
498 Frey, K. E., & Smith, L.C. (2007). How well do we know northern land cover?
499 Comparison of four global vegetation and wetland products with a new ground-truth

500   database for west Siberia. *Global Biogeochemical Cycles*, 21, GB1016,
501   doi:10.1029/2006GB002706.
502
503   Gamache, I. & Payette, S. (2005). Latitudinal response of subarctic tree lines to recent
504   climate change in eastern Canada. *Journal of Biogeography*, 32, 849-862.
505
506   Gessner, U., Conrad, C, Hüttich, C., Keil, M., Schmidt, M., Schramm, M., & Dech, S.
507   (2008). A multi-scale approach for retrieving proportional cover of life forms. IEEE
508   International Geoscience and Remote Sensing Symposium, 700-703.
509
510   Grace, J., Berninger, F., & Nagy, L. (2002). Impacts of climate change on tree line.
511   *Annals of Botany*. 90(4), 537-544.
512
513   Hagner, O., & Rigina, O. (1998). Detection of forest decline in Monchegorsk area.
514   *Remote Sensing of Environment*, 63(1), 11-23.
515
516   Hansen, M. C., Defries, R., Townshend, J., Carroll, M., Dimiceli, C., & Sohlberg, R.
517   (2003). Global percent tree cover at a spatial resolution of 500 meters: First results of the
518   MODIS vegetation continuous fields algorithm. *Earth Interactions*, 7, 1-15.
519
520   Hansen, J., Ruedy, R., Glascoe, J., & Sato, M. (1999). GISS analysis of surface
521   temperature change. *Journal of Geophysical Research*, 104, 30997-31022.
522   doi:10.1029/1999JD900835
523
524   Hansen, J., Sato, M., Ruedy, R., Lo, K., Lea, D.W., & Medina-Elizade, M. (2006).
525   Global temperature change. *Proceedings of the National Academy of Sciences*. 103 (39),
526   14288-14293.
527
528   Harding, R.J., Gryning, S.E., Halldin, S., & Lloyd, C.R. (2001). Progress in
529   understanding of land surface/atmosphere exchanges at high latitudes. *Theoretical*
530   *Applied Climatology*. 70, 5-18.
531
532   Heginbottom, J.A., J. Brown, E.S., Melnikov, & Ferrians, Jr., O.J. (1993). Circum-arctic
533   map of permafrost and ground ice conditions, *Proceedings of the Sixth International*
534   *Conference on Permafrost*, Wushan, Guangzhou, China: South China University Press,
535   Vol. 2: 1132-1136. Revised December 1997. Boulder, CO: National Snow and Ice Data
536   Center/World Data Center for Glaciology.
537
538   Heiskanen, J. (2008). Evaluation of global land cover data sets over the taiga–tundra
539   transition zone in northernmost Finland. *International Journal of Remote Sensing*,
540   29(13), 3727−3751.
541
542   Heiskanen, J. & Kivinen, S. (2008). Assessment of multispectral, -temporal and –angular
543   MODIS data for tree cover mapping in the tundra-taiga transition zone. *Remote Sensing*
544   *of Environment*, 112, 2367-2380.
545

546 Jorgenson, M.T., Shur, Y.L., & Pullman, E.R. (2006). Abrupt increase in permafrost
547 degradation in Arctic Alaska. *Geophysical Research Letters*. 33, L02503.
548 doi:10.1029/2005GL024960.
549
550 Kharuk, V.I., Dvinskaya, M. L., Ranson, K. J., Im, S. T. (2005). Expansion of evergreen
551 conifers to the larch-dominated zone and climatic trends. *Russian Journal of Ecology*,
552 36(3), 164-170.
553
554 Kharuk, V. I., Ranson, K. J., Tret'yakova, V., & Shashkin, E. A. (2002). Reaction of the
555 larch dominated communities on climate trends. In L. E. Paques (Ed.), Proceedings of an
556 International Symposium "Improvement of Larch (Larix sp.) for better growth, stem form
557 and wood quality". France Gap, September 16–21 (pp. 289– 295). INRA.
558
559 Kharuk, V. I., Shiyatov, S. G., Naurzbaev, M. M., & Fedotova, E. V. (1998). Forest–
560 tundra ecotone response to climate change. In Severin Woxhott (Ed.), Proceeding of
561 IBFRA-98 (pp. 19– 23). Oslo, Norway: Oslo, Sept 21–23.
562
563 Laliberté, A.C., & Payette, S. (2008). Primary succession of subarctic vegetation and soil
564 on the fast-rising coast of eastern Hudson Bay, Canada. *Journal of Biogeography, 35*,
565 1989-1999.
566
567 Lathrop, R.G., Montesano, P., & Haag, S. (2006). A multi-scale segmentation approach
568 to mapping seagrass habitats using airborne digital camera imagery. *Photogrammetric
569 Engineering & Remote Sensing*, 72(6), 665-675.
570
571 Lehner, B., & Doll, P. (2004). Development and validation of a global database of lakes,
572 reservoirs and wetlands. *Journal of Hydrology, 296*, 1-22.
573
574 Masek, J.G. (2001). Stability of boreal forest stands during recent climate change:
575 evidence from Landsat satellite imagery. *Journal of Biogeography, 28*, 967-976.
576
577 McMahon, G., Wiken, E.B., & Gauthier, D.A. (2004). Toward a scientifically rigorous
578 basis for developing mapped ecological regions. *Environmental Management, 34*, S111-
579 S124.
580
581 Montesano, P.M., Nelson, R., Sun, G., Margolis, H., Kerber, A., & Ranson, K.J. (2009).
582 MODIS tree cover validation for the circumpolar taiga-tundra transition zone. *Remote
583 Sensing of Environment*. 113, 2130-2141.
584
585 Olson, D.M., Dinerstein, E., Wikramanayake, E.D., Burgess, N.D., Powell, G.V.N.,
586 Underwood, E.C., D'Amico, J.A., Itoua, I., Strand, H.E., Morrison, J.C., Loucks, C.J.,
587 Allnutt, T.F., Ricketts, T.H., Kura, Y., Lamoreux, J.F., Wettengel, W.W., Hedao, P., &
588 Kassem, K.R. (2001). Terrestrial ecoregions of the worlds: A new map of life on
589 Earth. *Bioscience, 51*, 933-938.
590
591 Olthof, I., Pouliot, D., Latifovic, R., & Chen, W.J. (2008). Recent (1986-2006)

592   Vegetation-Specific NDVI Trends in Northern Canada from Satellite Data. *Arctic, 61*,
593   381-394.

594

595   Osterkamp, T.E., & Romanovsky, V.E. (1996). Characteristics of changing permafrost
596   temperatures in the Alaskan Arctic, USA. *Arctic and Alpine Research*. 28(3), 267-273.

597

598   Osterkamp, T.E., & Jorgenson, J.C. (2006). Warming of permafrost in the Arctic
599   National Wildlife Refuge, Alaska. *Permafrost and Periglacial Processes, 17*, 65-69.

600

601   Pavlov, A.V. (1994). Current changes of climate and permafrost in the arctic and sub-
602   arctic of Russia. *Permafrost and Periglacial Processes*. 5(2), 101-110.

603

604   Payette, S., Fortin, M.J., & Gamache, I. (2001). The subarctic forest-tundra: the structure
605   of a biome in a changing climate. *Bioscience*. 51(9), 709-718.

606

607   Payette, S. & Gagnon, R. (1985). Late Holocene deforestation and tree regeneration in
608   the forest-tundra of Quebec. *Nature,* 313, 570-572.

609

610   Pekkarinen, A. (2002). A method for the segmentation of very high spatial resolution
611   images of forested landscapes. *International Journal of Remote Sensing, 23*, 2817-2836.

612

613   Potapov, P., Yaroshenko, A., Turubanova, S., Dubinin, M., Laestadius, L., C. Thies, D.
614   Aksenov, A. Egorov, Y. Yesipova, I. Glushkov, M. Karpachevskiy, A. Kostikova, A.
615   Manisha, E. Tsybikova, and I. Zhuravleva. (2008). Mapping the world's intact forest
616   landscapes by remote sensing. *Ecology and Society*, 13(2), 51. URL:
617   http://www.ecologyandsociety.org/vol13/iss2/art51/

618

619   Ranson, K.J., Sun, G., Kharuk, V.I., & Kovacs, K. (2004). Assessing tundra-taiga
620   boundary with multi-sensor satellite data. *Remote Sensing of Environment, 93*, 283-295.

621

622   Rees, G., Brown, I., Mikkola, K., Virtanen, T., & Werkman, B. (2002). How can the
623   dynamics of the tundra-taiga boundary be remotely monitored? *Ambio*, 56-62.

624

625   Serreze, M.C., Walsh, J.E., Chapin III, F.S., Osterkamp, T., Dyurgerov, M.,
626   Romanovsky, V., Oechel, W.C., Morison, J., Zhang, T. & Barry, R.G. (2000).
627   Observational evidence of recent change in the northern high-latitude environment.
628   *Climate Change*, 46, 159-207.

629

630   Skre, O., Baxter, R., Crawford, R.M.M., Callaghan, T.V., & Fedorkov, A. (2002). How
631   will the tundra-taiga interface respond to climate change? *Ambio*, 12,37-46.

632

633   Stow, D.A., Hope, A., McGuire, D., Verbyla, D., Gamon, J., Huemmrich, F., Houston,
634   S., Racine, C., Sturm, M., Tape, K., Hinzman, L., Yoshikawa, K., Tweedie, C., Noyle,
635   B., Silapaswan, C., Douglas, D., Griffith, B., Jia, G., Epstein, H., Walker, D., Daeschner,
636   S., Petersen, A., Zhou, L.M., & Myneni, R. (2004). Remote sensing of vegetation and
637   land-cover change in Arctic Tundra Ecosystems. *Remote Sensing of Environment, 89*,

638 281-308.
639
640 Swann, A.L., Fung, I.Y., Levis, S., Bonan, G.B., & Doney, S.C. (2010). Changes in
641 Arctic vegetation amplify high-latitude warming through the greenhouse effect.
642 *Proceedings of the National Academy of Sciences*, 107(4), 1295-1300.
643
644 Sun, G., Ranson, K.J., Kharuk, V.I., & Kovacs, K. (2004). Changes in the taiga-tundra
645 boundary observed with Landsat. International Geoscience and Remote Sensing
646 Symposium Proceedings, *2004 IEEE International* 2 (2004), 722–724.
647
648 Tape, K., Sturm, M., & Racine, C. (2006). The evidence for shrub expansion in Northern
649 Alaska and the Pan-Arctic. *Global Change Biology,* 12, 686-702.
650
651 Tilton, J., Lawrence, W.T., & Plaza, A.J. (2006). Utilizing hierarchical segmentation to
652 generate water and snow masks to facilitate monitoring change with remotely sensed
653 image data. *GIScience & Remote Sensing,* 2006, 43(1), 39-66.
654
655 Timoney, K.P., La Roi, G.H., Zoltai, S.C., & Robinson, A.L. (1992). The high subarctic
656 forest-tundra of northwestern Canada: Position, Width, and Vegetation Gradients in
657 relation to climate. *Arctic,* 45(1), 1-9.
658
659 Timoney, K.P. (1995). Tree and tundra cover anomalies in the sub-arctic forest-tundra
660 and northwestern Canada. *Arctic,* 48(1), 13-21.
661
662 Toutoubalina, O.V., & Rees, W.G. (1999). Remote sensing of industrial impact on Arctic
663 vegetation around Noril'sk, northern Siberia: preliminary results. *International Journal of
664 Remote Sensing, 20*, 2979-2990.
665
666 van Aardt, J.A.N., Wynne, R.H., & Oderwald, R.G. (2006). Forest volume and biomass
667 estimation using small-footprint lidar-distributional parameters on a per-segment basis.
668 *Forest Science, 52*, 636-649.
669
670 Verbyla, D. (2008). The greening and browning of Alaska based on 1982-2003 satellite
671 data. *Global Ecology and Biogeography, 17*, 547-555.
672
673 Virtanen, T., Mikkola, K., Patova, E., & Nikula, A. (2002). Satellite image analysis of
674 human caused changes in the tundra vegetation around the city of Vorkuta, north-
675 European Russia. *Environmental Pollution, 120*, 647-658.
676
677 Vlassova, T.K. (2002). Human impacts on the tundra-taiga zone dynamics: The case of
678 the Russian lesotundra. *Ambio*, 30-36.
679
680 Walker, D.A., Raynolds, M.K., Daniels, F.J.A., Einarsson, E., Elvebakk, A., Gould,
681 W.A., Katenin, A.E., Kholod, S.S., Markon, C.J., Melnikov, E.S., Moskalenko, N.G.,
682 Talbot, S.S., Yurtsev, B.A., & Team, C. (2005). The Circumpolar Arctic vegetation map.
683 *Journal of Vegetation Science, 16*, 267-282.

684
685 Walker M.D., Wahren C.H., Hollister R.D. et al. (2006). Plant community responses to
686 experimental warming across the tundra biome. Proceedings of the National Academy of
687 Sciences, 103, 1342–1346.
688
689 Wulder, M.A., White, J.C., Cranny, M., Hall, R.J., Luther, J.E., Beaudoin, A.,
690 Goodenough, D.G., & Dechka, J.A. (2008). Monitoring Canada's forests. Part 1:
691 completion of the EOSD land cover project. *Canadian Journal of Remote Sensing.* 34(6),
692 549-562.

Tables

Table 1. Slope and y-intercept values of the linear adjustments for each circumpolar zone. Longitudes shown are the western and eastern bounds of each zone. Slope and y-intercept values based on results from Montesano et al. 2009.

Name	West	East	Slope	y - intercept
	Longitudinal Bounds			
Alaska	-180	-130	0.54	18.6
Western / Cent. Canada	-130	-80	0.53	24.58
Eastern Canada	-80	-55	0.66	10.96
Scandinavia	4	40	0.27	21.83
Western Eurasia	40	60	0.47	24.91
Central Eurasia	60	110	0.54	13.51
Eastern Eurasia	110	180	0.41	18.37

Table 2. Summary of the intersection of VCF_{adj} with CAVM and CAPI tree-lines. Regional longitudinal zone means are aggregated from 1° longitudinal zone means.

Name	Mean %TCC of 1° long. zones		Proportion of 1° zones with <5% mean %TCC	
	CAVM	CAPI	CAVM	CAPI
Alaska	7.3	8.1	0.43	0.46
Western / Cent. Canada	0.5	0.5	1.00	0.97
Eastern Canada	3.0	6.3	0.69	0.56
Scandinavia	---	6.2	---	0.60
Western Eurasia	23.0	7.9	0.00	0.45
Central Eurasia	10.9	11.8	0.45	0.37
Eastern Eurasia	6.7	6.2	0.63	0.58

Table 3. Area of both circumpolar ecotone classes broken down by regional zone. TTE Class 1 includes polygons with tree canopy cover of 5%-20%. TTE Class 2 includes polygons with <5% mean tree canopy cover and with a standard deviation of >5% mean tree canopy cover.

Name	TTE Class 1	TTE Class 2	Ratio: TTE Class 1 / TTE Class 2
	Area (sq. km.)		
Alaska	183,846	83,307	2.2
Western / Cent. Canada	305,032	35,756	8.5
Eastern Canada	123,155	35,172	3.5
Scandinavia	49,029	35,333	1.4
Western Eurasia	53,389	32,694	1.6
Central Eurasia	269,404	119,007	2.3
Eastern Eurasia	322,080	300,842	1.1
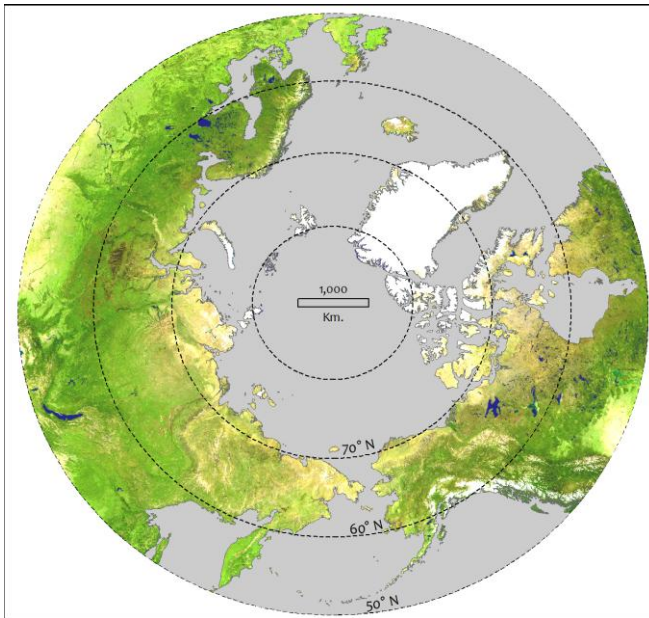
Figures

Figure 1. MODIS cloud free composite of the northern hemisphere in summer. The circumpolar taiga-tundra ecotone benchmarked in this study is about 13400km long.   Image source: earthobservatory.nasa.gov
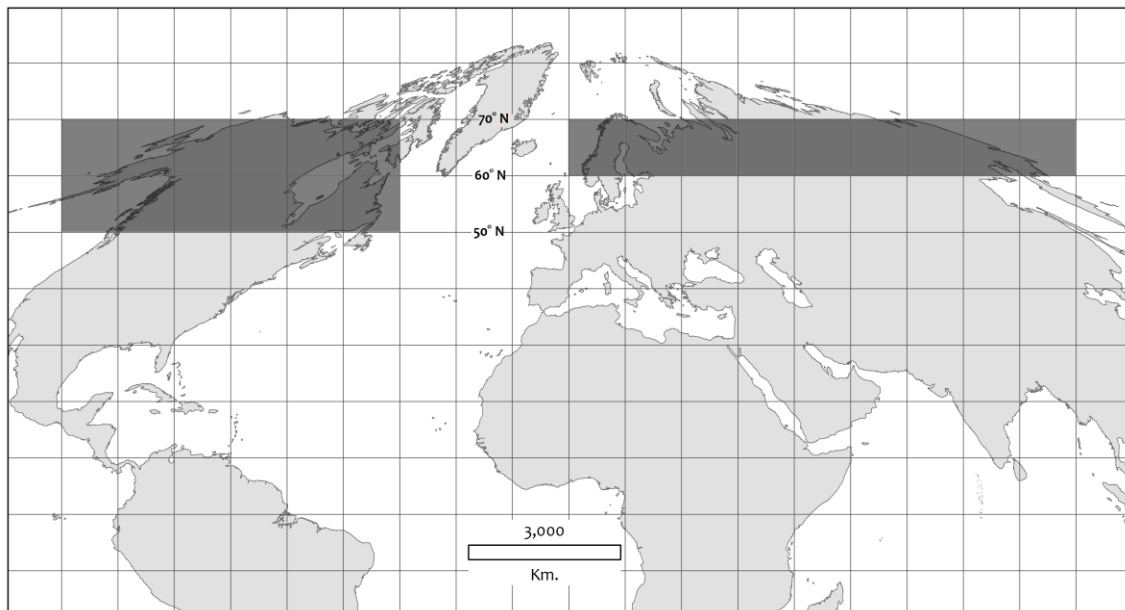

Figure 2. The 21 Collection 4 MODIS VCF tiles gathered for continental North America and Eurasia. Each tile is 10° X 10 ° and gridded in the sinusoidal projection.
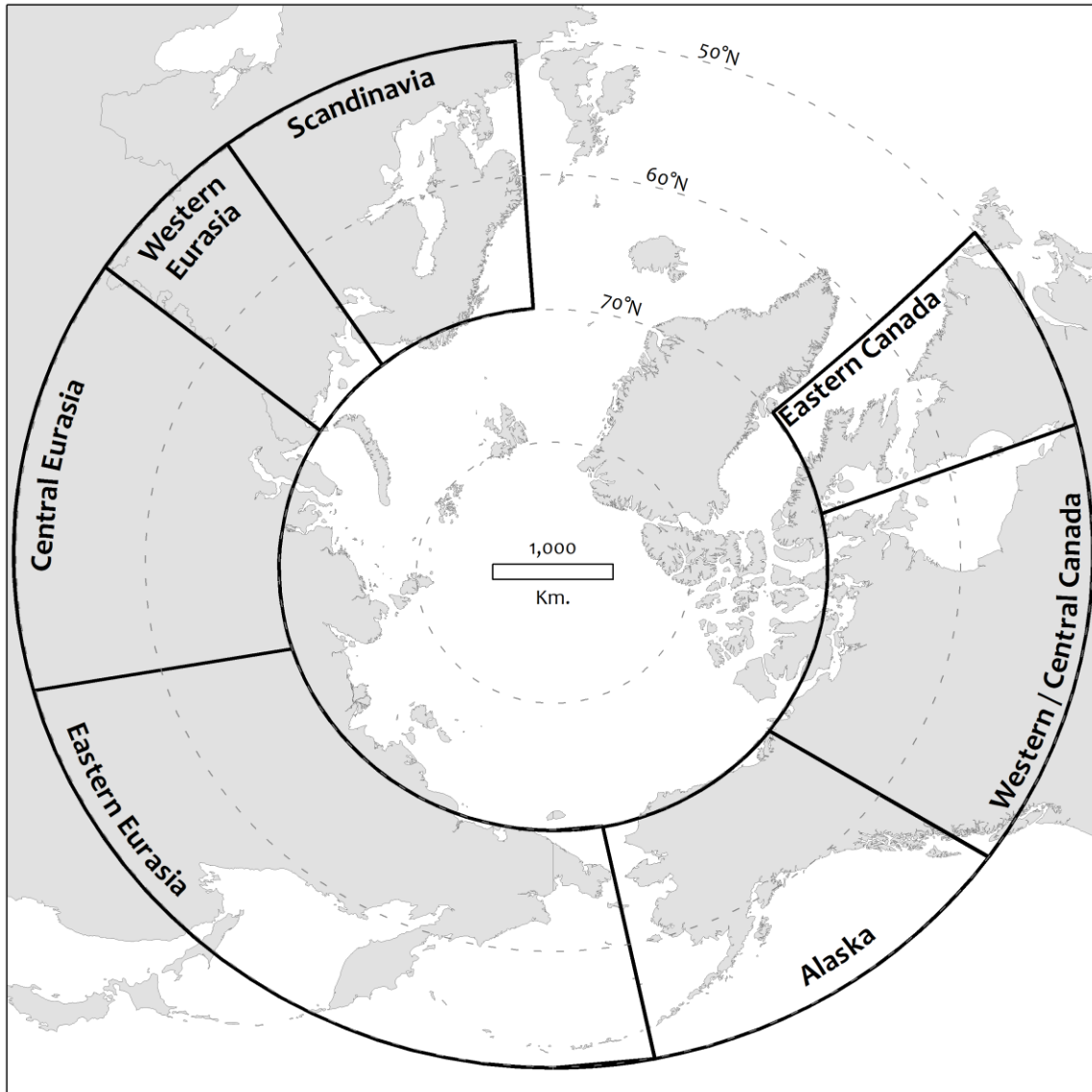
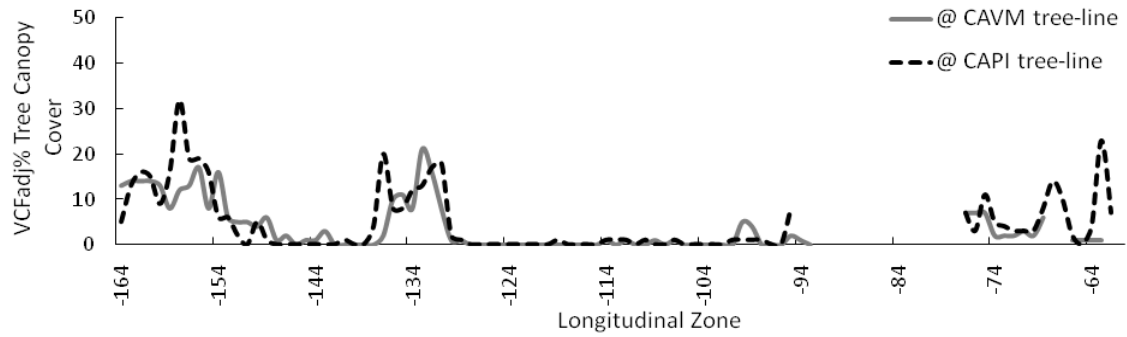**Figure 3. The 7 circumpolar zones by which linear equations adjusting VCF tree canopy cover values were applied.**

Figure 4a Mean VCF_{adj} values in each 1° longitudinal zone at the intersection with CAVM and CAPI tree lines in North America.
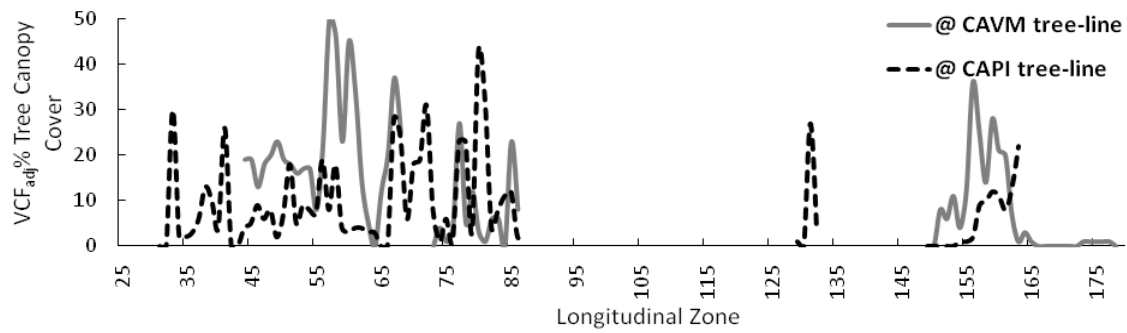
Figure 4b Mean VCF_{adj} values in each 1° longitudinal zone at the intersection with CAVM and CAPI tree lines in Eurasia.
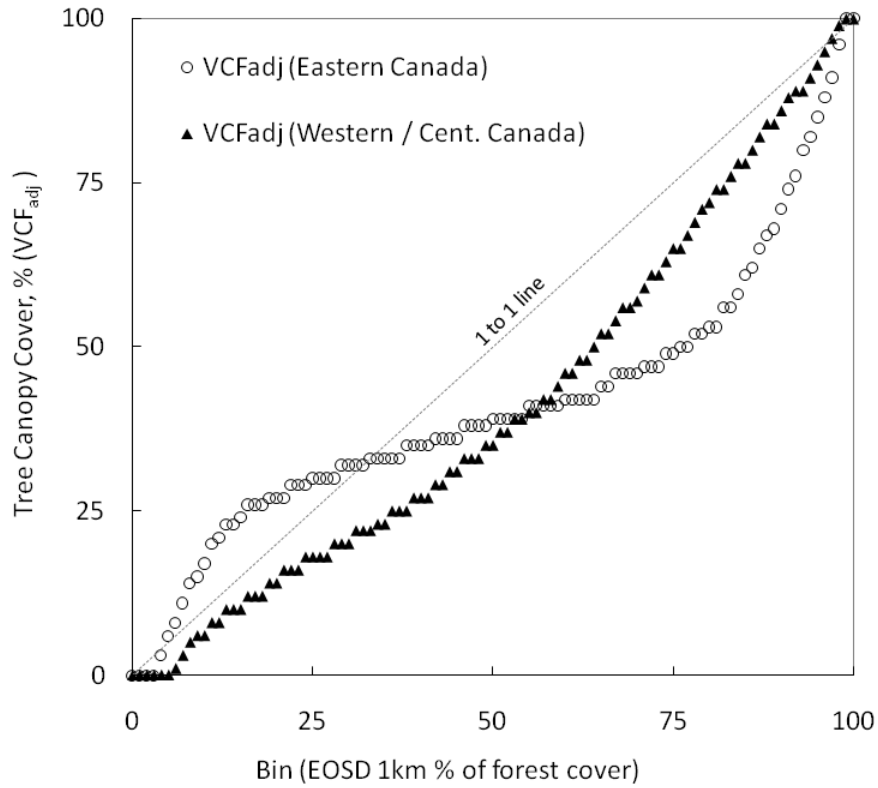
Figure 5. The median value of VCF$_{adj}$ %TCC for each bin of EOSD proportion of forest at 1% intervals.

Figure 6. The circumpolar taiga-tundra ecotone (TTE) map (6a). TTE Class 1 (red) depicts areas with a mean of 5-20% tree canopy cover and TTE Class 2 (blue) depicts areas of tree canopy cover <5% and standard deviation >5%. Dark green areas identify the boreal forest ecozone, light green areas are nonforest/ice/rock/tundra, and grey areas are those above 70 degrees N (no Collection 4 MODIS VCF data) or below 60 degrees (Eastern Hemsipher) or 50 degrees (Western Hemisphere). Figures 6 b-g depict larger scale versions of the 6a map, beginning in Alaska and moving to the east.
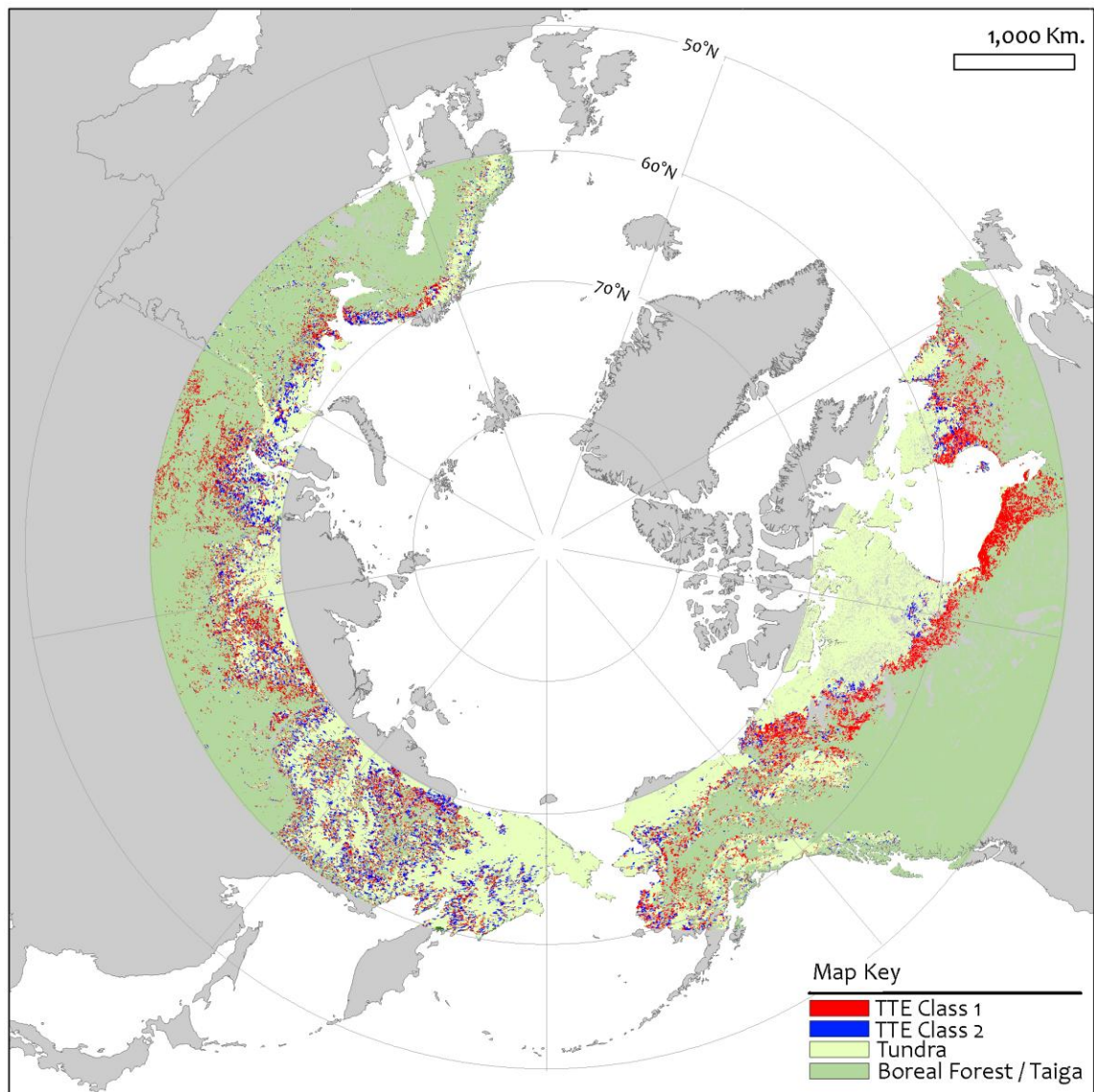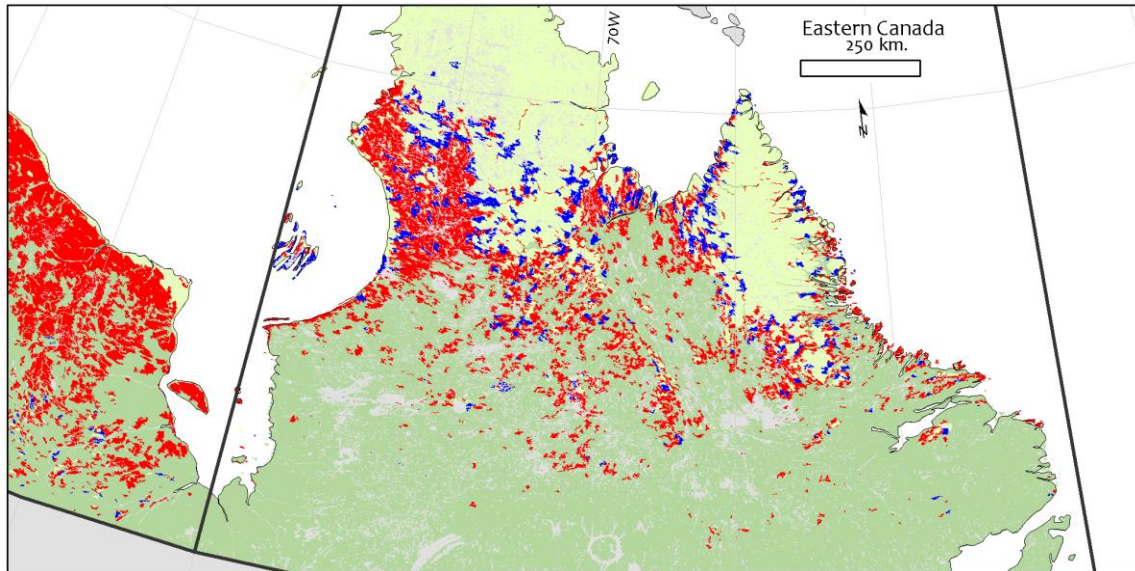
Figure 6a
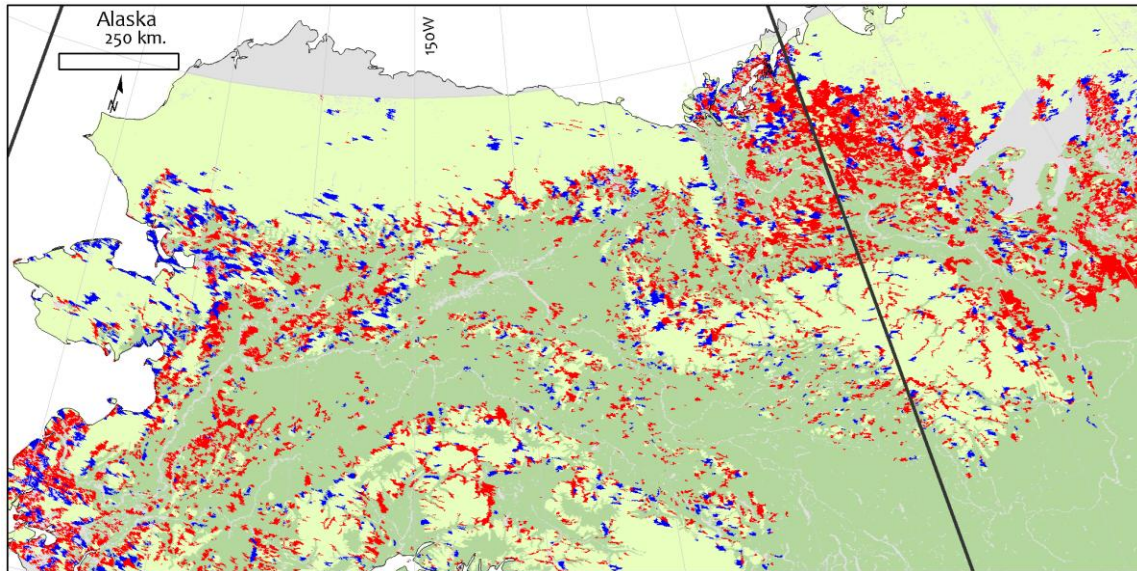
Figure 6b
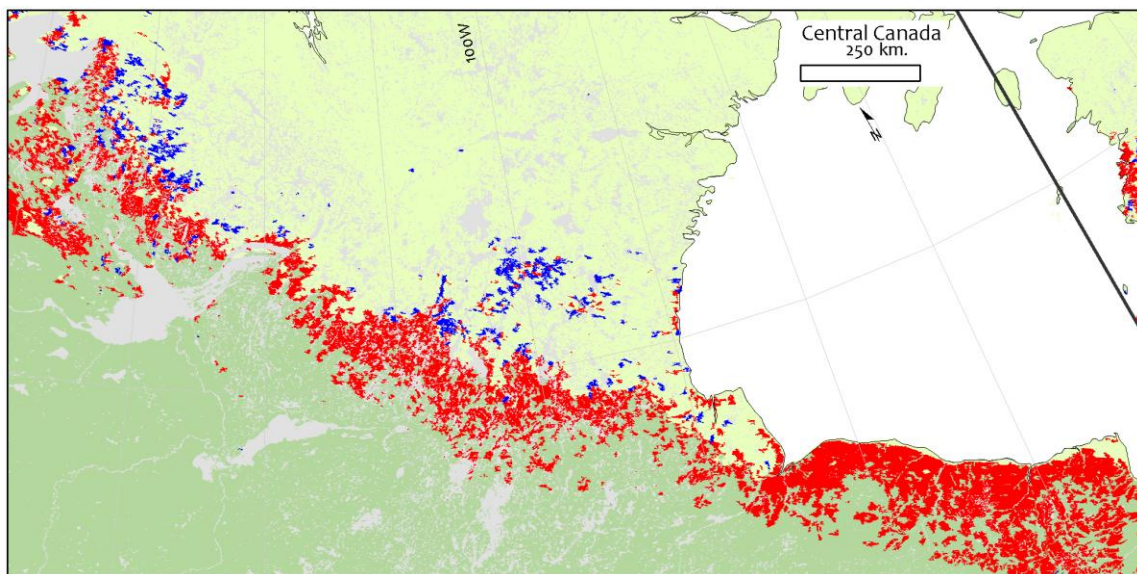
Figure 6c

Figure 6d
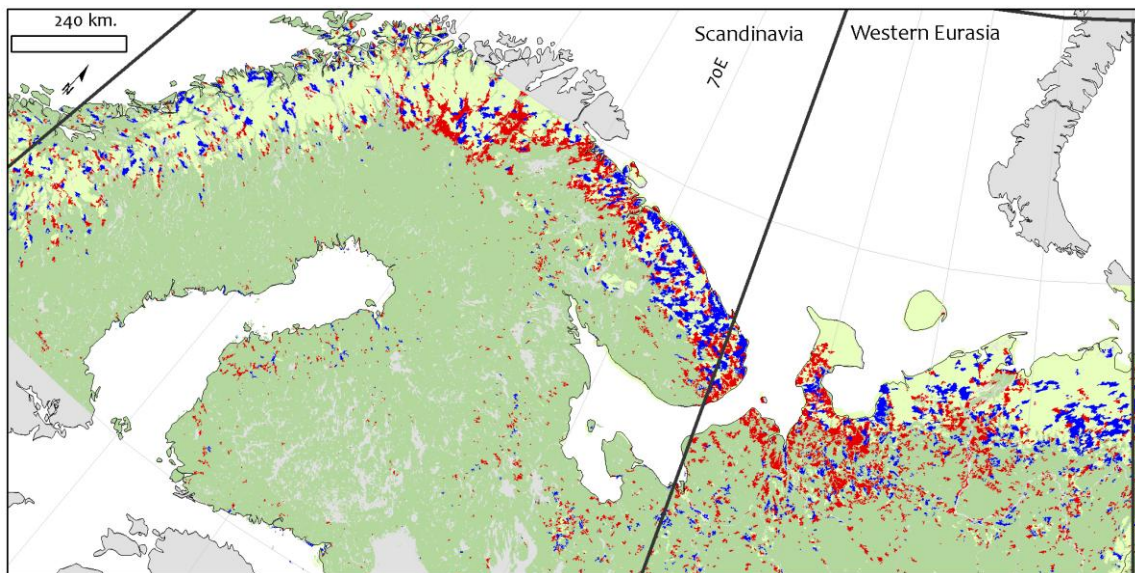
Figure 6e

Figure 6f

Figure 6g